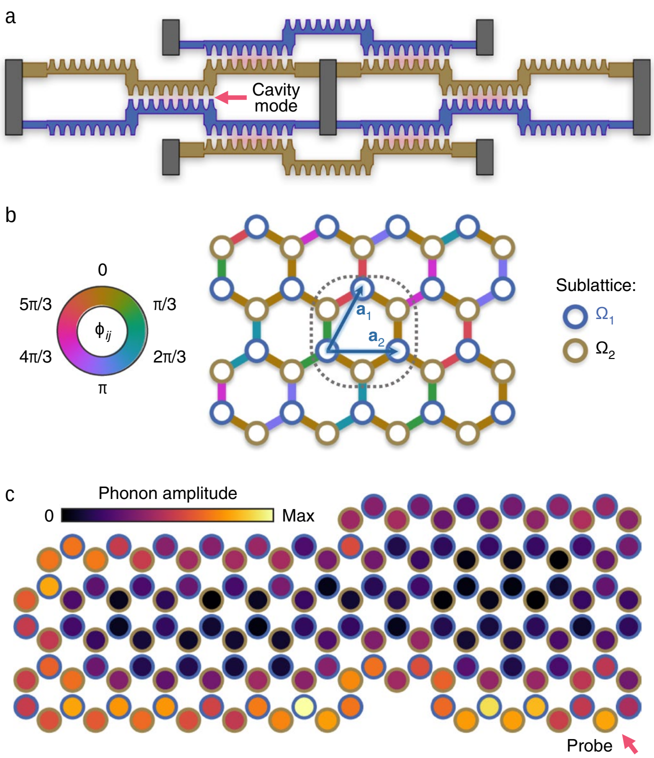

Fig. 4 | Extended optomechanical nanobeam lattice. a, Proposed experimental implementation of a topological nanobeam array. Nanobeams of different frequency are colour-coded, with grey rectangles depicting supports. Each nanobeam is interconnected to three nanobeams of different frequency via broadband nanophotonic cavities. **b**, This structure forms a honeycomb plaquette (surrounded by a dashed line), where each circle denotes an entire arm. By repetition, a honeycomb lattice with primitive lattice vectors is formed. The optical modulation phases to create a specific topological insulator phase, defined in the text, are indicated by the colours of the links. **c**, Simulated steady-state phononic amplitude under continuous driving, focused on the site indicated by an arrow. Chosen parameters are $\Gamma_1\ 2\pi = \Gamma_2\ 2\pi = 4\ 5$ kHz, $_{\mathrm{eff}}\ 2\pi = 200$ kHz, phononic frequency disorder with standard deviation $\sigma_\Omega\ 2\pi = 20$ kHz and direct mechanical coupling of t $\pi =$ kHz.

Non-trivial topological properties are then observed for rational ($= 1\ 3$ in the following), where the bandstructure for an infinite ribbon geometry shows q bulk bands split into q ◻ gaps, traversed by (chiral) counter-propagating edge modes (see top panel in Extended Data Fig. 2c). To exemplify phononic propagation along the boundary of a finite array, we calculate the steady state while driving an edge site (see Methods). A moderate frequency disorder of ◻ % is introduced, in addition to direct mechanical coupling of □ t2 hi ji2n n n l¼1 2ðbl ðiþy bl ðjþ þ h c þ linking next-nearest neighbours[26]. As shown by the calculated amplitudes in Fig. 4c, emerging phononic edge modes display unidirectional propagation within state-of-the-art fabrication tolerances (see Supplementary Section III and Extended Data Fig. 2c–e for more details). This demonstrates a feasible platform for nanoscale phononic topological insulators based on optically induced magnetic fields.

In conclusion, we have established a synthetic gauge field for nanomechanical transport using optically mediated couplings in an optomechanical system. We have introduced an experimental platform with large optomechanical interactions and bandwidths that unlocks many-mode implementations in the nanomechanical domain. The tunability of our system allows the investigation of physics beyond the rotating wave approximation and in synthetic dimensions[31]. Out-of-plane optical control provides a counterpart to electromechanical methods[32,33] with unique traits. It offers prospects for exploring the impact of thermal and quantum fluctuations on topologically protected phonon transport[21] and the effects of mechanical or optomechanical nonlinearities[26]. It is an advance towards exploiting topologically protected sound in the quantum acoustics regime and the search for exotic states such as those produced by non-Abelian gauge fields and analogues of the fractional quantum Hall effect[30] in the realm of nanomechanics.

Online content

Any methods, additional references, Nature Research reporting summaries, source data, extended data, supplementary information, acknowledgements, peer review information; details of author contributions and competing interests; and statements of data and code availability are available at https://doi.org/10.1038/s41565-019-0630-8.

Received: 16 January 2019; Accepted: 18 December 2019;
Published online: 03 February 2020

References

1. Laughlin, R. B. Quantized Hall conductivity in two dimensions. *Phys. Rev. B* **23**, 5632 (1981).
2. Peano, V., Brendel, C., Schmidt, M. & Marquardt, F. Topological phases of sound and light. *Phys. Rev. X* **5**, 031011 (2015).
3. Ruesink, F., Miri, M.-A., Alù, A. & Verhagen, E. Nonreciprocity and magnetic-free isolation based on optomechanical interactions. *Nat. Commun.* **7**, 13662 (2016).
4. Fang, K. et al. Generalized non-reciprocity in an optomechanical circuit via synthetic magnetism and reservoir engineering. *Nat. Phys.* **13**, 465–471 (2017).
5. Aharonov, Y. & Bohm, D. Significance of electromagnetic potentials in the quantum theory. *Phys. Rev.* **115**, 485–491 (1959).
6. Ozawa, T. et al. Topological photonics. *Rev. Mod. Phys.* **91**, 015006 (2019).
7. Goldman, N., Budich, J. & Zoller, P. Topological quantum matter with ultracold gases in optical lattices. *Nat. Phys.* **12**, 639–645 (2016).
8. Huber, S. D. Topological mechanics. *Nat. Phys.* **12**, 621–623 (2016).
9. Lindner, N. H., Refael, G. & Galitski, V. Floquet topological insulator in semiconductor quantum wells. *Nat. Phys.* **7**, 490–495 (2011).
10. Dalibard, J., Gerbier, F., Juzeliūnas, G. & Öhberg, P. Colloquium: Artificial gauge potentials for neutral atoms. *Rev. Mod. Phys.* **83**, 1523–1543 (2011).
11. Bermudez, A., Schaetz, T. & Porras, D. Synthetic gauge fields for vibrational excitations of trapped ions. *Phys. Rev. Lett.* **107**, 150501 (2011).
12. Fang, K., Yu, Z. & Fan, S. Photonic Aharonov–Bohm effect based on dynamic modulation. *Phys. Rev. Lett.* **108**, 153901 (2012).
13. Fang, K., Yu, Z. & Fan, S. Realizing effective magnetic field for photons by controlling the phase of dynamic modulation. *Nat. Photon.* **6**, 782–787 (2012).
14. Nash, L. M. et al. Topological mechanics of gyroscopic metamaterials. *Proc. Natl Acad. Sci. USA* **112**, 14495–14500 (2015).
15. Wang, Y. et al. Observation of nonreciprocal wave propagation in a dynamic phononic lattice. *Phys. Rev. Lett.* **121**, 194301 (2018).
16. Cha, J., Kim, K. W. & Daraio, C. Experimental realization of on-chip topological nanoelectromechanical metamaterials. *Nature* **564**, 229–233 (2018).
17. Shen, Z. et al. Experimental realization of optomechanically induced non-reciprocity. *Nat. Photon.* **10**, 657–661 (2016).
18. Peterson, G. A. et al. Demonstration of efficient nonreciprocity in a microwave optomechanical circuit. *Phys. Rev. X* **7**, 031001 (2017).
19. Bernier, N. R. et al. Nonreciprocal reconfigurable microwave optomechanical circuit. *Nat. Commun.* **8**, 604 (2017).
20. Xu, H., Mason, D., Jiang, L. & Harris, J. Topological energy transfer in an optomechanical system with exceptional points. *Nature* **537**, 80–83 (2016).
21. Xu, H., Jiang, L., Clerk, A. A. & Harris, J. G. E. Nonreciprocal control and cooling of phonon modes in an optomechanical system. *Nature* **568**, 65–69 (2019).
22. Walter, S. & Marquardt, F. Classical dynamical gauge fields in optomechanics. *New J. Phys.* **18**, 113029 (2016).
23. Shkarin, A. et al. Optically mediated hybridization between two mechanical modes. *Phys. Rev. Lett.* **112**, 013602 (2014).
24. Weaver, M. J. et al. Coherent optomechanical state transfer between disparate mechanical resonators. *Nat. Commun.* **8**, 824 (2017).

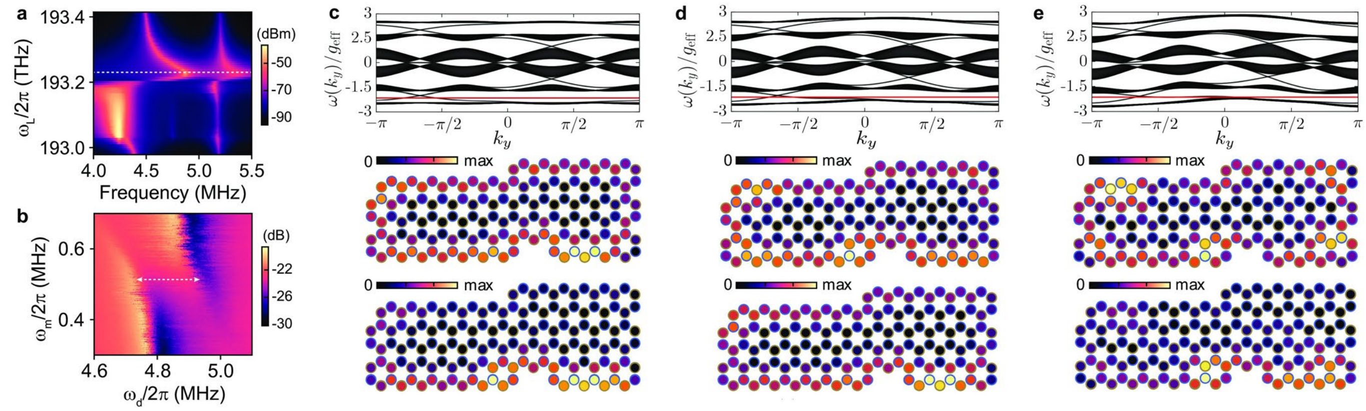

Extended Data Fig. 2 | Robust phononic edge states. a, Optical spring shift measured at higher optical powers for a separate device shows large tunability of the mechanical modes. The dashed, white line shows the drive laser detuning used in b. The unusual features between 193.0 and 193.2 THz are due to a dynamically unstable regime of potential photothermoelastic origin. **b**, The modulated coupling strength, geff, is higher for higher optical powers. The largest modulated coupling strength measured in our experiments is marked by the dashed line and seen to be 2 × 200 kHz. Here the detection laser was absent and the drive laser response was directly demodulated using the lock-in amplifier leading to a Fano shaped feature for the driven response. **c**,**d**,**e**, (top panels) Band structure for a ribbon geometry (width L = 20) for increasing values of the direct mechanical coupling from left to right (0, 10, and 20 kHz, respectively), displaying the driving modulation frequency. The steady-state phononic amplitude in the absence of disorder is displayed in the middle row, while the result with a phononic frequency disorder with standard deviation σ π = 20 kHz (averaged over 100 realizations) is shown at the bottom. For these plots, = .